9th AIAA/ISSMO Symposium and Exhibit on Multidisciplinary Analysis and Optimization AIAA-2002-5668

OPTIMIZED UNMANNED AERIAL VEHICLE WITH WING MORPHING FOR EXTENDED RANGE AND ENDURANCE

Shawn E. Gano * **John E. Renaud** †

Department of Aerospace and Mechanical Engineering
University of Notre Dame
Notre Dame, Indiana
Email: John.E.Renaud.2@nd.edu

Abstract

Due to their current successes, unmanned aerial vehicles (UAVs) are becoming a standard means of collecting information. However, as their missions become more complex and require them to fly farther, UAVs can become large and expensive due to fuel needs. Sidestepping the paradigm of a fixed static wing, the variform concept developed in this paper allows for greater fuel efficiency. Bulky wings could morph into sleeker profiles, reducing drag, as they burn fuel. The development of such wings will rely heavily on computational design exploiting state of the art optimization techniques that account for uncertainty and insure reliability.

Nomenclature

α	Angle of attack
η	Propeller efficiency
ρ_∞	Free stream density
c	Specific fuel consumption
C_D	Drag coefficient
C_L	Lift coefficient
D	Total drag
E	Endurance
P	Engine power
P_A	Power available
P_R	Power required
R	Range
S	Planform Area
t	Time
T	Thrust
T_R	Thrust required
V_∞	Free stream velocity
W_1	Weight of aircraft without fuel and with full payload
W_0	Weight of aircraft with full fuel and payload
W_f	Weight of fuel

1 Introduction

Unmanned aerial vehicles (UAVs) are being used more frequently in all parts of the world today. This type of vehicle can take on many different missions, ranging from the conducting of scientific experiments to intelligence gathering surveillance during the day or night. They are

*Graduate Research Assistant, Student Member AIAA
†Professor, Associate Fellow AIAA.

capable of undertaking missions from 50 hours, like IAI Malat's Heron, to fractions of an hour. In every case the range and endurance of the craft is limited by its storage capacity for fuel. In most cases, especially for surveillance missions, an increase of mission range and endurance without the addition of heavy fuel is greatly desired.

The problem is that UAVs today have already been optimized for their current mission objectives. Thus, in order to conduct longer missions, more fuel and, hence, the size of the aircraft would need to be increased. In this proposal, a new paradigm is described that could allow these craft greater range without requiring them to carry more fuel. Alternatively, they could carry less fuel than current models and still achieve the same objectives.

In order to improve the fuel efficiency of UAVs, we propose using a wing that changes its shape during flight to minimize total mission drag. This wing morphing[18] approach is referred to as the *variform wing concept*. The fuel would be stored in balloon-like bladders inside the wing structure. These bladders would shrink as the fuel is consumed. A bladder's size and shape, as well as the possibility of multiple bladders in a wing, will be determined by optimization techniques. The integrated bladder and elastic structure of the wing provide a truly multidisciplinary problem that involves aerodynamics, structures, and controls.

There are other classes of aircraft that could also benefit from the variform concept, such as micro aerial vehicles (MAVs). However, in this paper we will focus on applications and examples involving UAVs.

The variform concept presented here differs from other current research, like that done by NASA's Aircraft Morphing Program[18], which uses piezoelectric to induce shape changes. The use of piezoelectrics has been mostly for control[11,17]. They are using them to rapidly change the shape of the trailing edge of the wings in place of ailerons (or in some cases to change the shape of the whole wing). The variform concept as presented here is to use the consumption of fuel to slowly change the shape of the entire wing throughout the flight to lower the drag on the craft over the entire mission.

Research being done at the Naval Research Laboratory (NRL) also deals with structure-plus-power concepts[19]. Their program has three main design concepts. Their first concept is replacing some of the passive structure of smaller MAVs with with battery material. More simply stated, they incorporate the battery as a structural member of the craft, so the weight of the battery is somewhat offset by lowering the weight of the structural components needed. A second NRL idea uses autophagous structure-fuel components. In this case the structure itself would be a fuel source, so the aircraft would self-consume structure over the course of the mission. Their last concept is another type of variform structure-power idea. In this case the structural members of the wing would be inflated with fuel. The first two concepts conserve constant aerodynamic shapes and thus are not very similar to the work presented in this paper. The third concept is similar in that the aerodynamic shape is altered via the fuel supply. However, the variform concept that is presented in this paper does not restrict the fuel to be inflated into structural members or in any certain configuration, but allows for an optimization process to choose where and how the structure should deform.

In this paper the variform concept is introduced in more detail, along with a description of the research that has been completed and an outline of future work. Initial efforts have focused on the development of a computational fluid dynamics model for predicting aerodynamic forces and performance. Future efforts will include the development of a finite element model of the bladder-filled elastic wing structure. The CFD and FEA codes will then be integrated to form a multidisciplinary model of the variform concept. Shape optimization techniques will be used to

optimize the uninflated airfoil geometry and the uninflated bladder geometry. The optimization will seek to maximize the variform UAV's range while accounting for system uncertainties. The model will allow users to explore different structural materials and variform design concepts.

2 Typical UAV Description

To provide a better understanding of the UAV class of aircraft, this section covers the main aspects of the AAI Corporation's Shadow.

The Shadow is a small stealthy monoplane powered by a pusher engine. It has two tail booms and an inverted V tail. It is composed of mainly graphite and Kevlar epoxy composites. The optional tricycle landing gear is detachable. The Shadow typically caries either a video camera, electro-optical camera, or an infra-red sensor. Hence, it is primarily used for surveillance and target acquisition. The craft can be controlled either by pre-programming or via remote control and can be launched by conventional means or by a hydraulic catapult. It can carry about 40 liters of fuel, has a wing span of about 4 m, and can be up to 149 kg at launch[9]. AAI's Shadow is depicted both in flight and during launch in Figure 1.

Figure 1. AAI Shadow UAV launch (left) and in flight (right).

The Shadow exhibits the typical performance characteristics of UAVs[9]. It can cruise at a maximum speed of 156 km/h and has a flight ceiling resulting from the fuel to air mixture in the engine of 4,575 m. The craft can operate for about 5-6 hours with one tank of fuel and has an operational radius of about 125 km.

3 The Variform Concept

The variform wing is simply a wing that changes shape as fuel is consumed in order to maximize the lift to drag ratio. Maximizing this ratio leads to a great increase in the range of the aircraft. It is a way of making the aircraft go substantially further on the same amount or less fuel. For example, say we start with a NACA 23015 wing cross-section. As the fuel is used up, the wing could morph into the shape of a FX 60-126. This is captured in Figure 2, where the outside line is the larger NACA airfoil and the inner solid section is the sleeker shape.

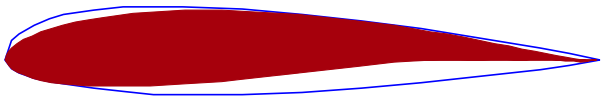

Figure 2. Variform Wing Concept

This shape changing could be done in a variety of ways. One way this change could occur would be to store the fuel in balloon like bladders that interact with the structure of the wing. When the bladders are filled the shape would look like the outer profile in Figure 2, and when empty the shape would look like the inner solid-filled shape. The simplest bladder configuration, as shown in Figure 3A, would just be an oval or any simple geometric shape. However, to achieve greater control of how the wing changes over time, a non-symmetric shape could be used as the bladder (Figure 3B), or even possibly multiple bladders of different size and shape seen in part C of the same figure.

3.1 MDO Problem Description

The variform wing concept will require an elastic wing structure capable of satisfying conventional UAV structural concerns. At the same

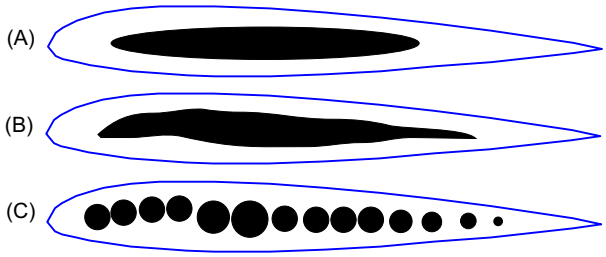

Figure 3. Possible Fuel Bladder Configurations.

time the variform wing's elastic structure must accommodate the shape deformations induced by the pressurized fuel filled bladder. The analysis of the variform wing involves a coupled fluid-structure analysis of the wings' geometry throughout the mission. In addition, one needs to perform a conventional aeroelastic analysis of the wing. A number of structural issues such as rigidity and the integrity of the wing will need to be addressed concurrently. Additionally, the fuel control, or pressurization of the fuel bladders, needs to be taken into account. This is due to the fact that there may be a certain sequence in which the airfoil should deform to achieve the maximal performance. The design procedure should insure that the design is consistent for this complex coupled system. Figure 4 illustrates the coupled system analysis.

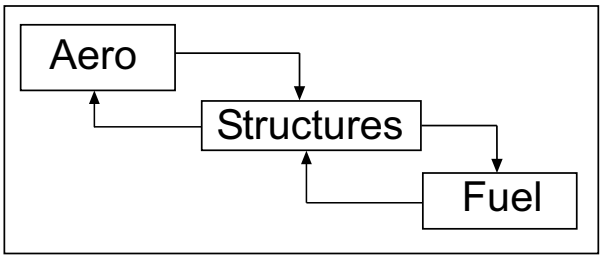

Figure 4. Variform MDO Problem

The design objective is to maximize the range or endurance of the UAV. System constraints may include climb rates and gradients, stability, maximum weights, as well as any other performance or structural limitations desired. This could easily be written in the standard form:

$$\begin{aligned} \underset{\mathbf{x}}{\text{maximize}}: \quad & R(\mathbf{x}) \\ \text{subject to}: \quad & \mathbf{l} \leq \begin{pmatrix} \mathbf{x} \\ \mathbf{Aero}(\mathbf{x}) \\ \mathbf{Struct}(\mathbf{x}) \\ \mathbf{Contr}(\mathbf{x}) \end{pmatrix} \leq \mathbf{u} \end{aligned}$$

Where $\mathbf{x}$ are the design variables, $\mathbf{l}$ and $\mathbf{u}$ are the upper and lower bounds respectively, and $\mathbf{Aero}(\mathbf{x})$, $\mathbf{Struct}(\mathbf{x})$, and $\mathbf{Contr}(\mathbf{x})$ are aerodynamic, structural, and control constraints, respectively.

The full MDO problem would include design variables for each node that defines the airfoil and bladder shapes (as seen in Figure 5) or the parameters needed to describe the shapes of the airfoil and the bladders[20]. Additional design variables could include maximum takeoff weight, cruise altitudes, and thrust.

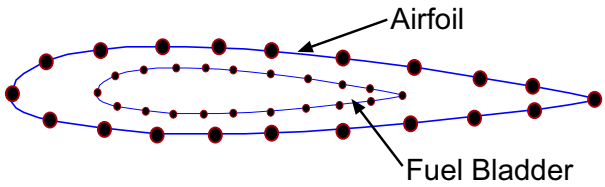

Figure 5. Variform Parametrization

Once the analysis model is completed, optimization methods could be employed to search out the most efficient wing sections and determine how they evolve throughout the flight. Methods such as Adaptive Experimental Design[14] (AED) could be used because of their CPU savings. Further, massively paralleled computers would be used for their time savings. One could apply Reliability Based Design Optimization[8] (RBDO) to find the best design to account for uncertainties in the system.

3.2 Range and Endurance Improvement Estimates

For a conceptual qualification of the savings of the variform concept, first consider two airfoils.

The first airfoil has a thicker cross-section and the second has a sleeker profile. The only other constraint of these two airfoils is that the smaller airfoil must fit entirely inside the larger one. Next, we find the aerodynamic properties of these two shapes, either through wind tunnel experiments or CFD simulations (or both). The drag polar for each airfoil might look like the initial and final airfoil lines depicted in Figure 6. The diagram shows that the initial airfoil has a higher drag coefficient at every corresponding lift coefficient. This may not be the case everywhere in the drag polars but should be a general trend.

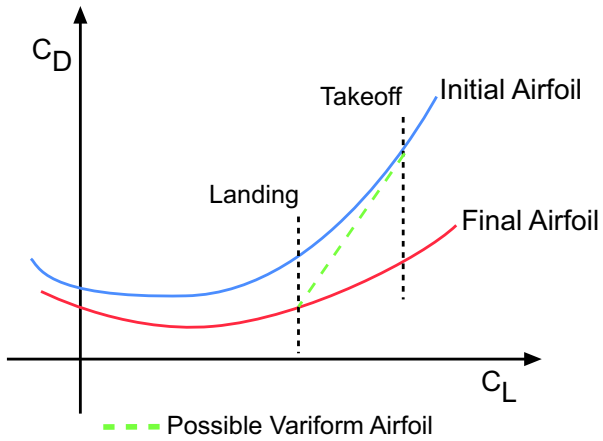

Figure 6. The drag polar of the initial, final, and predicted variform airfoils.

Next, assume that the aircraft only looses weight via fuel consumption. This is not an essential assumption, but it is more for convenience to avoid discontinuities. Further, most missions will be of this type for UAVs. This means that there are defined takeoff and landing weights, with corresponding coefficients of lift. These two values for lift are also drawn in Figure 6.

Finally, if our wing started off in the shape of the thicker airfoil and as the craft used up the fuel supply, the wing morphed into the shape of the thinner airfoil, then the drag polar of this aircraft would be different than each of the other airfoils. Let us assume that this wing's drag polar runs between the two airfoils and again, for simplicity, just follows a straight line between the two. In the example problem at the end of the paper we investigate further where the actual drag polar lies. Using the Breguet equations[2] for propeller powered aircraft that assume steady level flight, the range and endurance equations are:

$$R = \frac{\eta}{c}\frac{C_L}{C_D}\ln\left(\frac{W_0}{W_1}\right), \tag{1}$$

$$E = \frac{\eta}{c}\frac{C_L^{3/2}}{C_D}\frac{\sqrt{2\rho_\infty S}}{\sqrt{W_1}-\sqrt{W_0}}. \tag{2}$$

Of all the parameters in Equations 1 and 2, the only values that are not constant are the lift and drag coefficients. For this qualitative estimate we will just take the average values of lift and drag coefficients over the mission. The average lift is about the same for all the airfoils, but the drag for the variform wing is significantly less than that of its non-shape-changing counterpart the thicker airfoil. From looking at experimental data of low Reynolds number airfoils[12,15] this savings could be in the range of 15 to 30 percent.

3.2.1 Range and Endurance Equations

The Breguet equations used in the previous section serve well only for very rough estimates for the true range or endurance of an aircraft and have many assumptions in their derivations. A few of these assumptions are valid for typical aircraft but are not as applicable for an aircraft with variform wings. However, they do provide a good reference point. In this section we derive from first principles more accurate equations for analyzing the morphing wings so that we can better quantify the range and endurance gain.

The weight of fuel consumed over a time change of Δt is defined as $c \cdot P \cdot \Delta t$. Therefore, the differential change in weight due to fuel consumption is $c \cdot P \cdot dt$. Considering that, the weight of the aircraft is defined as:

$$W_1 = W_0 - W_f. \tag{3}$$

Here we assume that the only changes in weight involve the fuel weight change and that the weight decreases with time. Thus:

$$dW_f = dW = -cPdt. \tag{4}$$

Rearranging Equation 4 and integrating both sides, time between 0 and the endurance E, and weight between W_o (full fuel) and W_1 (fuel empty), gives:

$$\int_0^E \mathrm{d}t = -\int_{W_0}^{W_1} \frac{1}{cP}\mathrm{d}W. \tag{5}$$

From this we get an expression for the endurance:

$$E = \int_{W_1}^{W_0} \frac{1}{cP}\mathrm{d}W. \tag{6}$$

To find the range, we multiply Equation 4 by V_∞ and note that $V_\infty dt$ is a differential distance dx. This gives:

$$V_\infty dt = dx = -\frac{V_\infty dW}{cP}. \tag{7}$$

Integrating both sides from $x = 0$ to the final range R and the same weights as before produces:

$$\int_0^R \mathrm{d}x = -\int_{W_0}^{W_1} \frac{V_\infty}{cP}\mathrm{d}W. \tag{8}$$

Therefore an expression for the range is:

$$R = \int_{W_1}^{W_0} \frac{V_\infty}{cP}\mathrm{d}W. \tag{9}$$

At this point, in order to simplify the equations for range and endurance, we introduce one assumption. We assume that the entire mission is level unaccelerated flight. This would be a good assumption for an aircraft that was trying to maximize its range or endurance. From this assumption, the thrust required is equal, to the drag of the craft: $T_R = D$. Also, the power required is equal so the trust required times the free stream velocity is: $P_R = T_R V_\infty$. Combining these two equalities yields:

$$P_R = T_R V_\infty = DV_\infty. \tag{10}$$

By definition, the total power of the engine is equal to the power required divided by the efficiency of the propeller. Combining this fact with Equation 10 gives:

$$P = \frac{P_R = P_A}{\eta} = \frac{DV_\infty}{\eta}. \tag{11}$$

Substituting the previous result into the range equation (Equation 9) simplifies to:

$$R = \int_{W_1}^{W_0} \frac{\eta}{cD}\mathrm{d}W. \tag{12}$$

Because of our assumption of steady level flight $W = L$, we can multiply the right hand side of Equation 12 by $\frac{L}{W}$ to get:

$$R = \int_{W_1}^{W_0} \frac{L}{D}\frac{\eta}{c}\frac{\mathrm{d}W}{W}. \tag{13}$$

Further noting that $L/D = C_L/C_D$, we get our final expression for the range:

$$R = \int_{W_1}^{W_0} \frac{C_L}{C_D}\frac{\eta}{c}\frac{\mathrm{d}W}{W}. \tag{14}$$

Using the same procedure for simplifying the endurance equation yields:

$$E = \int_{W_1}^{W_0} \frac{\eta}{c}\frac{C_L}{C_D V_\infty}\frac{\mathrm{d}W}{W}. \tag{15}$$

However, this expression can be simplified one step further using $L = W = \frac{1}{2}\rho_\infty V_\infty^2 S C_L$, solving for V_∞, and subsituting that into Equation 15 to get the final endurance equation:

$$E = \int_{W_1}^{W_0} \frac{\eta}{c}\frac{C_L^{3/2}}{C_D}\sqrt{\frac{\rho_\infty S}{2}}\frac{\mathrm{d}W}{W^{3/2}}. \tag{16}$$

4 Example Case: Flying Wing

To demonstrate the level of range and endurance gained in using the variform concept, we present here a simple example. This example is not a best case or worst case scenario but rather just a pseudo random example to see if and how much can be gained by using this new approach.

This example considers a flying wing that has a large aspect ratio and is in steady level flight from takeoff to landing. This assumption is made to make the analysis simpler. Using these assumptions we can just analyze the airfoil cross-section properties while not worrying about drag from the airframe body or other three dimensional effects. This is a simplification from a real-world UAV; however, it does maintain key aspects which make this a reasonable model for testing out this new concept.

For this example the airfoils shown in Figure 2, specifically, the NACA 23015 morphing into the FX 60-126, are used. The flying wing was modelled using parameters of the Shadow UAV which was introduced in a previous section. The flight conditions were established at an altitude of 3,000 km, Reynolds number of 1×10^6, and at a cruising speed, V_∞ = 33.7 m/s. Using the near maximum takeoff weight for the craft, which must equal the lift, we calculate a lift coefficient, $C_L = 1.1$. Likewise at landing, subtracting the fuel weight gives: $C_L = 0.89$.

For the airfoil analysis a computational fluid dynamics code, called CFL3D v6.0, developed at NASA's Langley Research Center was used. CFL3D is a Reynolds-Averaged thin-layer Navier-Stokes flow solver for structured grids[10]. The algorithms employed within CFL3D solve the time-dependent conservation law form of the Reynolds-averaged Navier-Stokes equations. A semi-discrete finite-volume approach is used in spatial discretization[10]. The convective pressure terms use upwind-biasing. Central differencing is employed for the shear stress and heat transfer terms. Implicit time advancement is used, allowing for the solving of both steady and unsteady flows. CFL3D version 6.0 features a new ability to obtain a solution for a specific lift coefficient (C_L). For this case the angle of attack (α) is not known and is considered part of the desired solution. Therefore the analysis of the airfoil cross-sections will be able to predict drag and allow for runs when the coefficient of lift is known instead of the angle of attack (as in the case of the variform wing).

The first step of the analysis varies the angle of attack for the initial and final airfoil shapes to construct a drag polar for each. Each drag polar is shown in Figure 7. Also shown in the figure are the takeoff and landing lift coefficients.

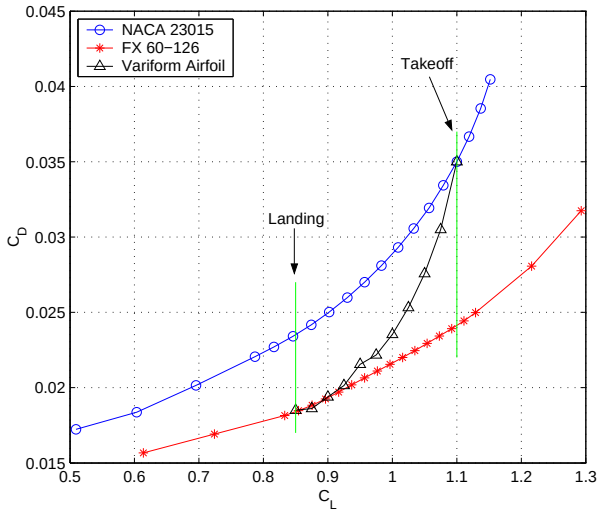

Figure 7. Drag Polars from CFD Simulations

The next step was to linearly morph the shape of the larger airfoil to the smaller airfoil. Then, using each corresponding intermediate lift coefficient, the variform airfoil's drag polar was constructed. A linear morph was used purely as a convenience, since no optimization to find the best shape change over time was done in this example. Thus, the final result could be improved by such an optimization. The results are plotted in Figure 7. The streamline flow solutions for both the takeoff and landing conditions are shown in Figures 8 and 9, respectively.

Once all this data was computed and collected, the range and endurance was found for both the variform and the NACA 23015 airfoils using the Equations 14 and 16, which were derived in Section 3.2.1. It is assumed that both the specific fuel consumption and the propeller efficiency were constant throughout the flight. The results showed

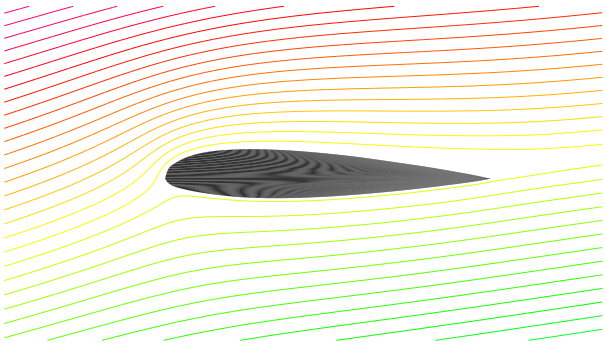

Figure 8. Takeoff, $C_L = 1.1$

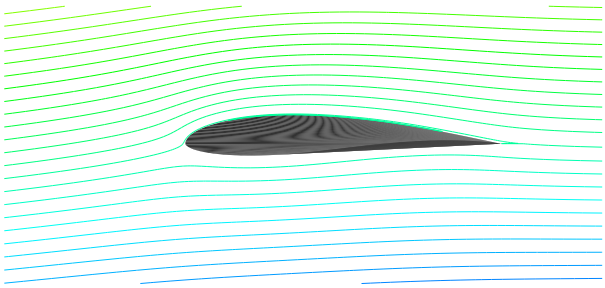

Figure 9. Landing $C_L = 0.85$

that the range of the of the variform wing was 22.3% further and the endurance was 22.0% longer than the initial static NACA airfoil.

5 Conclusions and Future Research

Even with no optimization done on the variform wing in this example case, the range and endurance increase was within the expected range. The increase in both distance and time was quite significant and would greatly benefit many UAV missions.

The example case shows that the variform concept readily extends missions and therefore, a more complete model and analysis should be completed. The work illustrated in this paper lays the foundation for further progress on this topic and shows that the concept is worth more investigation.

Further work should be directed towards developing a structural model and finding suitable materials that will allow for this deformation with the needed stiffness. Building the full coupled MDO analysis and parameterizing the outer airfoil shape and inner bladder shape also need further study.

The majority of the research remaining for this morphing wing design will be in developing the rest of the software model for the complete system analysis and then employing optimization methods that account for uncertainty[8] to produce a robust variform wing with maximized range.

Once all the systems have been modelled and integrated, this MDO problem could also serve as a test problem for comparing different optimization methods.

Acknowledgments

This multidisciplinary research effort is supported in part by the following grants and contracts; NSF grants DMI98-12857 and DMI01-14975, NASA grant NAG1-2240. Thank you Rebekah Hauch and Jessica Hauch (undergraduate research assistants) for helping run the example case.

References

1.- Abbott, I.H., Von Doenhoff, A.E.: *Theory of Wing Sections*, Dover, 1959.

2.- Anderson, J.D., *Introduction to Flight*, McGraw-Hill, 1989.

3.- Belegundu, A.D., Chandrupatla, T.R: *Optimization Concepts and Applications in Engineering*, Prentice Hall, 1999.

4.- Biedron R.T: *CFL3D Version 6.0*, http://cfl3d.larc.nasa.gov/Cfl3dv6/cfl3dv6.html, December 18, 2001.

5.- Fletcher, C.A.J.: *Computational Techniques for Fluid Dynamics*, vol 1, Springer, 1991.

6.- Fletcher, C.A.J.: *Computational Techniques for Fluid Dynamics*, vol 2, Springer, 1991.

7.- Forster, E., Livne, E., *Integrated Structure/Actuation Synthesis of Strain Actuated Devices for Shape Control*, Proceedings of the 42st AIAA/ASME/ASCE/AHS/ASC Structures, Structural Dynamics, and Materials Conference, AIAA 2001-1621, Seattle, WA, April 16-19.

8.- Gu, X., Renaud, J.E., Batill, S.M., Brach, R.M., Budhiraja, A.S., *Worst Case Propagated Uncertainty of Multidisciplinary Systems in Robust Design Optimization*, Structural and Multidisciplinary Optimization, Vol.20, No.3, pp.190-213, Published by Springer-Verlag, 2000.

9.- Jane's Online, *Jane's Unmanned Aerial Vehicles and Targets*, AAI RQ-7A Shadow 200, accessed April 12, 2001.

10.- Krist, S.L., Biedron, R.T.: *CFL3D User's Maual (Version 5.0)*, NASA/TM-1998-208444, 1998.

11.- Anna-Maria R. McGowan, Lucas G. Horta, Joycelyn S. Harrison and David L. Raney, *Research Activities Within NASA's Morphing Program*, NATO-RTO Workshop on Structural Aspects of Flexible Aircraft Control, Ottawa, Canada, October 18-21, 1999.

12.- Miley, S.J., *A Catalog of Low Reynolds Number Airfoil Data For Wind Turine Applications*, February 1982.

13.- Sharon L. Padula, James L. Rogers and David L. Raney, *Multidisciplinary Techniques and Novel Aircraft Control Systems*, 8th AIAA/NASA/USAF/ISSMO Multidisciplinary Analysis and Optimization Symposium, Long Beach, California, AIAA 2000-4848, September 6-8, 2000, pp. 11.

14.- Pérez, V. M., Renaud, J.E., Watson, L. T., 2001, *Adaptive Experimental Design for Construction of Response Surface Approximations*, Proceedings of the 42nd AIAA/ASME/ASCE/AHS/ASC Structures, Structural Dynamics, and Materials Conference, AIAA 2001-1622, Seattle, WA, April 16-19.

15.- Selig, M.S., Donovan, J.F., Fraser, D.B.: *Airfoils at Low Speeds*, Soartech 8 H. A. Stokely, 1989.

16.- Sorenson, R.L: *A Computer Program to Generate Two-Dimensional Grids About Airfoils and Other Shapes by the Use of Poisson's Equation*, NASA Technical Memorandum 81198, 1980.

17.- J. O. Simpson, S. A. Wise, R. G. Bryant, R. J. Cano, T. S. Gates, , J.A. Hinkley, R.S. Rogowski and K. S. Whitley,*Innovative Materials for Aircraft Morphing*, SPIE'S 5th Annual International Symposium on Smart Structures and Materials, San Diego, CA, March 1-5, 1998, pp. 10.

18.- R. W. Wlezien, G. C. Horner, A. R. McGowan, S. L. Padula, M. A. Scott, R. J. Silcox and J. O. Simpson, *The Aircraft Morphing Program*, 39th AIAA/ASME/ASCE/AHS/ASC Structures, Structural Dynamics, and Materials Conference, Long Beach, California, AIAA 98-1927, April 20-23, 1998.

19.- Naval Research Laboratory (James P. Thomas), *Structural Performance with Energy Storage for Air Vehicles Through Multifunctional Design and Fabrication*, http://mstd.nrl.navy.mil/6350/MfM.html, December 14, 2001.

20.- Vanderplaats, G.N.: *Numerical Optimization Techniques for Engineering Design*, McGraw-Hill, 1984.